



Prediction of the soil–water characteristic curves for the fine-grained soils with different initial void ratios

Qian Zhai¹ · Yiyao Zhu¹ · Harianto Rahardjo² · Alfrendo Satyanaga³ · Guoliang Dai¹ · Weiming Gong¹ · Xueliang Zhao¹ · Yazhou Ou⁴

Received: 7 July 2022 / Accepted: 8 February 2023 / Published online: 8 April 2023
© The Author(s), under exclusive licence to Springer-Verlag GmbH Germany, part of Springer Nature 2023

Abstract

Soil–water characteristic curve (SWCC) contains the key information related to the hydromechanical properties of unsaturated soil. It is noted that the shapes of the SWCC for the fine-grained soils could be different if the specimens were prepared with different initial void ratios. The pore structure of soil is altered when the specimen experiences mechanical or suction loading. Determination of a group of SWCCs for different specimens through the experimental measurement is time-consuming and costly. In this paper, a new method is proposed to predict the SWCCs for the fine-grained soil with different initial void ratios. The measured SWCC in the form of gravimetric water content (SWCC-*w*) for the specimen with a high void ratio and the volumetric shrinkage curve is adopted as the input information. The SWCC-*w* for the specimen with another void ratio is subsequently estimated using the proposed method in this paper. The estimated results from the proposed method in this paper show a good agreement with the experimental data from the published literature. The proposed method provides an alternative method for the prediction of the SWCC for the fine-grained soil with different initial void ratios.

Keywords Fine-grained soil · Pore size distribution function (PSDF) · Soil–water characteristic curve (SWCC) · Volumetric shrinkage curve (VSC)

1 Introduction

Fredlund [8] indicated that the soil–water characteristic curve (SWCC), which reflects the capacity of water storage and other unsaturated soil properties, was commonly viewed as necessary input information for the numerical

modeling in solving the geotechnical problems. Researchers such as Mualem, Fredlund et al., Fredlund et al., Zhai and Rahardjo and Zhai et al. [4, 6, 16, 31, 33] illustrated the methodology in the estimation of hydraulic conductivity and shear strength of unsaturated soil from the SWCC. Many researchers [11–13, 28] reported that different SWCCs could be obtained when the soil specimens are prepared with different initial void ratios. Normally, the SWCC measurement is time-consuming for the fine-grained soil because of its low coefficient of permeability (or hydraulic conductivity). Considering both cost- and time-consuming, it is impractical to most engineers and researchers to determine the group of SWCCs for the same soil with different initial void ratios by relying on the experimental measurements. In addition, it seems that the mechanism associated with the different SWCCs for the specimens with different initial void ratios has not been well investigated. Therefore, a predictive model with the theoretical background is urgently needed for the

✉ Qian Zhai
101012332@seu.edu.cn

¹ Key Laboratory of Concrete and Prestressed Concrete Structures of Ministry of Education, Southeast University, Nanjing 210096, China
² School of Civil and Environmental Engineering, Nanyang Technological University, Block N1, Nanyang Ave., Singapore 639798, Singapore
³ Department of Civil and Environmental Engineering, School of Engineering and Digital Sciences, Nazarbayev University, Kabanbay Batyr Ave., 53, 010000 Nur-Sultan, Republic of Kazakhstan
⁴ China Construction Eighth Engineering Division Co., LTD, Shanghai, China

description of SWCC variation with respect to a change in the initial void ratio.

In this paper, a new method is proposed for the prediction of the SWCCs corresponding to different initial void ratio. In the proposed method, both measured SWCCs in the form of gravimetric water content (SWCC- w) for the soil with high void ratio and the volumetric shrinkage curve (VSC) are adopted as the input information in the proposed method. Subsequently, the SWCC- w for the specimen with a lower void ratio is predicted using the proposed method. The prediction results from the proposed method in this paper were verified with experimental data from the published literature. The proposed method provides an indirect method rather than direct measurements for the determination of SWCCs for the soil with different initial void ratios.

2 Literature review

The works from Vanapalli et al., Ng and Pang and Tarantino [19, 24, 28] indicated that the SWCC for the fine-grained soil could exhibit different shapes depending on the stress history and initial void ratio. Tang et al. and Rostami et al. [22, 25] conducted numbers of measurements and observed that the water storage capacity of soil (or SWCC) was mainly affected by the variation in void ratio for the specimen. Through a large number of experimental data, Gallipoli [10] observed that the slopes of SWCCs for the soil with different initial void ratios remain constant in high-suction range. Fredlund and Houston [9] explained that SWCC in the form of degree of saturation (SWCC- S) could be calculated from the measured SWCC- w and VSC. They also observed that converted SWCCs- S from different SWCCs- w and VSC yielded the same curve. The works from Lee et al., Tavakoli et al., Millard et al., Garakani et al., and Pasha et al. [11, 13, 17, 20, 26] indicated that the difference in SWCC would further affect the determination of the shear strength and hydraulic conductivity for the unsaturated soil. A predictive model for an indirect determination of a group of SWCCs with different initial void ratios is of great importance for the implementation of the principles of unsaturated soil mechanics in the practical engineering.

Romero et al. [21] adopted techniques of mercury intrusion porosimetry (MIP) and scanning electron microscopy (SEM) to study the soil structure and analyze the shrinkage of aggregated fabric for the clayey soil. Through the MIP tests for specimens with different initial void ratios, Nowamooz and Masrouri [18] observed that the pore size distributions had similar shapes for the pore range greater than 10^{-1} μm and the pore size distributions overlap each other for the pore range less than 10^{-1} μm . Rostami

et al. [22] considered the changes of pores and soil-throat under different net stresses and proposed a method to determine the SWCCs for the soil under various stress conditions. But in this model, the ratio of throat to pore radius needs to be calibrated by using the experimental data. From the results of MIP tests, Sun and Cui [23] proposed to predict the SWCC by analyzing the law of deformation of pores. Bate et al. [2] proposed a new method to estimate the SWCC by incorporating the variation of the pores based on the technique of the digitized image algorithm. Zhai and Rahardjo [31] indicated that SWCC- S can be considered as the integration of the pore size distribution function (PSDF) for the soil with negligible volume change. Zhai et al. [34] improved the conventional capillary model, which was presented by Millington and Quirk [15] and Mualem [16], and proposed a modified capillary model by simplifying the irregular pores into a series of circular pores with different sizes. By using the improved capillary model, PSDF can be converted from SWCC- S . Zhai et al. [35] illustrated that the variation of the PSDF for the soil which had undergone volume change in the drying process and proposed a framework to estimate this variation from the measured SWCC- w and VSC. In this paper, the method from Zhai et al. [35] was adopted and further improved for the prediction of SWCCs for the specimens with different initial void ratios.

There are several equations including but not limited Brooks and Corey, van Genuchten and Fredlund and Xing [1, 6, 27] for the description of the SWCC. Most of those SWCC equations are proposed mainly for the unimodal SWCC. Zhang and Chen [30] and Zhai et al. [32] illustrated that Fredlund and Xing [5] equation could also be used for the representation of a bimodal SWCC through the best-fitting technique. In addition, Yan et al. [29] developed a framework for the description of the multimodal SWCC. Fredlund and Xing's equation [5], as illustrated in Eq. (1), is considered as one of most popular SWCC equations and has been using by researchers. Therefore, Fredlund and Xing's equation [5] is adopted for representation of SWCC- w in this paper. Meanwhile, Fredlund et al.'s equation [7], as shown in Eq. (2), was adopted for the representation of the volumetric shrinkage curve.

$$w(\psi) = \left[1 - \frac{\ln\left(1 + \frac{\psi}{C_r}\right)}{\ln\left(1 + \frac{10^6}{C_r}\right)} \right] \frac{w_s}{\left\{ \ln\left[e + \left(\frac{\psi}{a}\right)^n \right] \right\}^m} \quad (1)$$

where $w(\psi)$ is the gravimetric water content at the soil suction of ψ ; w_s is the saturated gravimetric water content; a , m , n are the fitting parameters; and C_r is the input parameter for the rough estimation of the residual suction.

$$e(w) = a_{sh} \left(\frac{w^{c_{sh}}}{b_{sh}^{c_{sh}}} + 1 \right)^{\frac{1}{c_{sh}}} \tag{2}$$

where $e(w)$ is the void ratio corresponding to the gravimetric water content of w and a_{sh} , b_{sh} and c_{sh} are the fitting parameters.

3 Theory

Based on the improved capillary model from Zhai et al. [34], the pores in soil can be divided into a series of groups of pores with different radii. The pores in the fine-grained soil are divided into different fractions. It is known that PSDF changes gradually when the soil undergoes the volume change. However, the variation of PSDF can be predicted if the PSDFs corresponding to several instantaneous states have been obtained. In this paper, the changes of the fractions at different instantaneous states are calculated from the measured SWCC- w and VSC. The SWCCs for the specimens with different initial void ratios are predicted by considering the variation of PSDF of soil.

3.1 Effect of matric suction on the pore deformation

Due to the difference in the value of pore-air pressure and pore-water pressure, the air–water interface forms a curve, called the meniscus which has a contact angle $(\frac{\pi}{2} - \alpha)$ to the surface of soil particles, as shown in Fig. 1a. Through the capillary law, a meniscus shows a corresponding radius of R . The surface tension (T) of the air–water interface balances the difference in the pore-air and the pore-water pressures. Meanwhile, the curved air–water interface transfers the load (reactive stress, T' , of the surface tension, T) to the soil structure which hold the meniscus. T' can be divided into two components in both x and z directions, such as T'_z which results in additional compression to the

soil structure and T'_x which leads to capillary bonding between soil particles, as illustrated in Fig. 1b. The compression stress on the soil structures can be calculated by multiplying the suction with the projected area of the meniscus in z direction while the capillary bonding (or pulling stress) between particles A and B can be calculated by multiplying the suction with the projected area of the meniscus in y direction. As shown in Fig. 1b, the projected area of the meniscus on the xz plane is a shape of sector and its area is defined as A' . As a result, the pulling stress (P_s) between particles A and B can be calculated using Eq. (3) as follows:

$$P_s = (u_a - u_w)A' = (u_a - u_w) \left(R^2\alpha - r\sqrt{R^2 - r^2} \right) \tag{3}$$

where u_a is the pore-air pressure, u_w is the pore-water pressure, $u_a - u_w$ is the matric suction, R is the radius corresponding to matric suction, r is the radius of the pore and α is an angle determined by R and r ($\alpha = \arcsin(r/R)$).

It is noted that radius R represents the soil suction while the r represents the pore in the soil. A larger R represents a lower soil suction. If $R\sin\alpha$ is lower than r , then air can penetrate the pore with radius of r . When the R is much larger than r ($R \gg r$), then the pulling stress (P_s) calculated from Eq. (3) approaches zero. In other words, the pulling stress resulted from the meniscus could not compress the pores when the radius of the pore is much smaller than the radius of the meniscus.

Based on the improved capillary model, the pores in a soil are divided into several groups for the entire suction from 0.01 to 10^6 kPa. Define the pore radii for the groups from the largest to the smallest as $r_1, r_2, r_3, \dots, r_i, \dots, r_n$. When the suction increases to ψ_i which is corresponding to the value of r_i based on the capillary law, the pores with radii much smaller than r_i will not be compressed by the pulling stress as shown in Eq. (3).

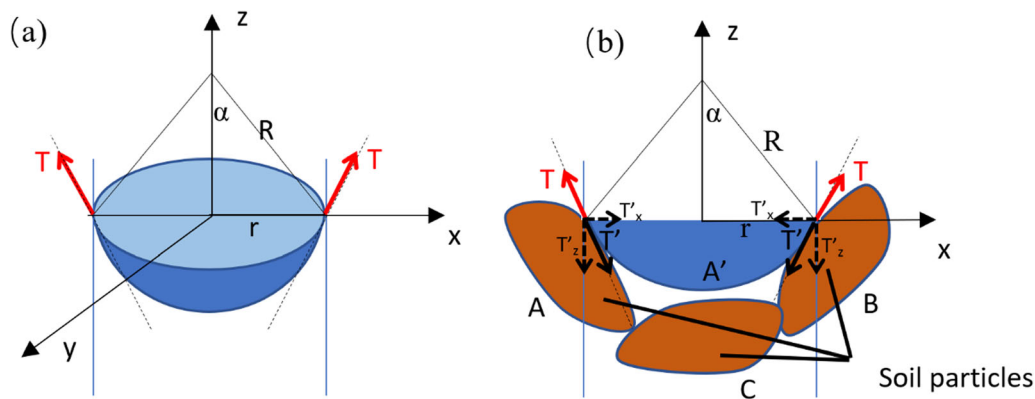


Fig. 1 a Illustration of the surface tension on the meniscus; b Illustration of the stress transferred to the soil structure from the meniscus

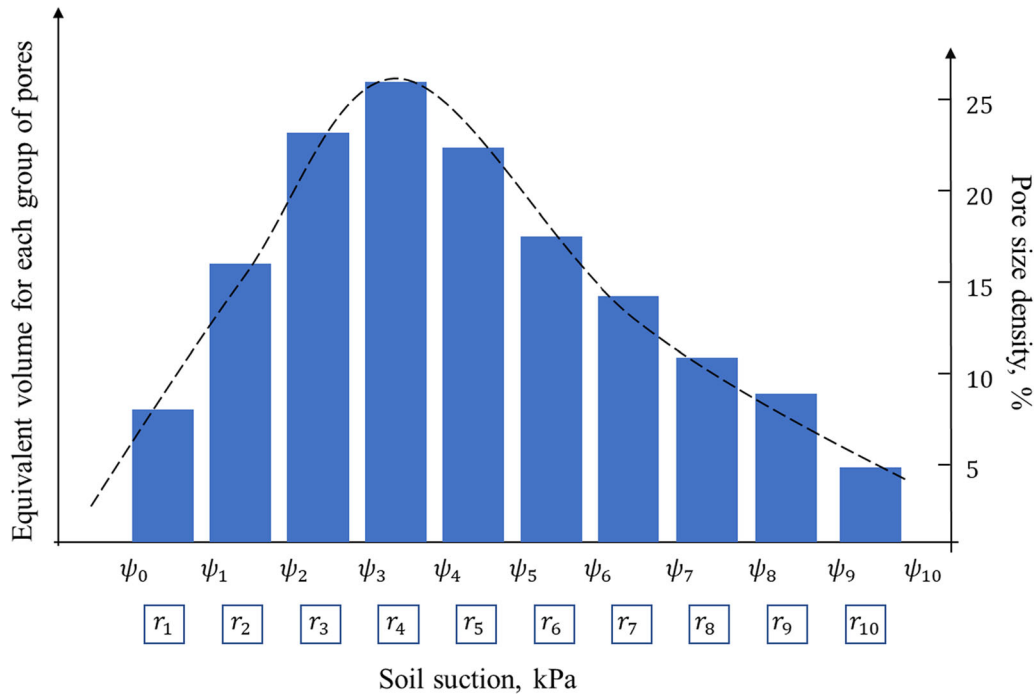


Fig. 2 Illustration of the pore fractions in soil corresponding to the void ratio of e_0

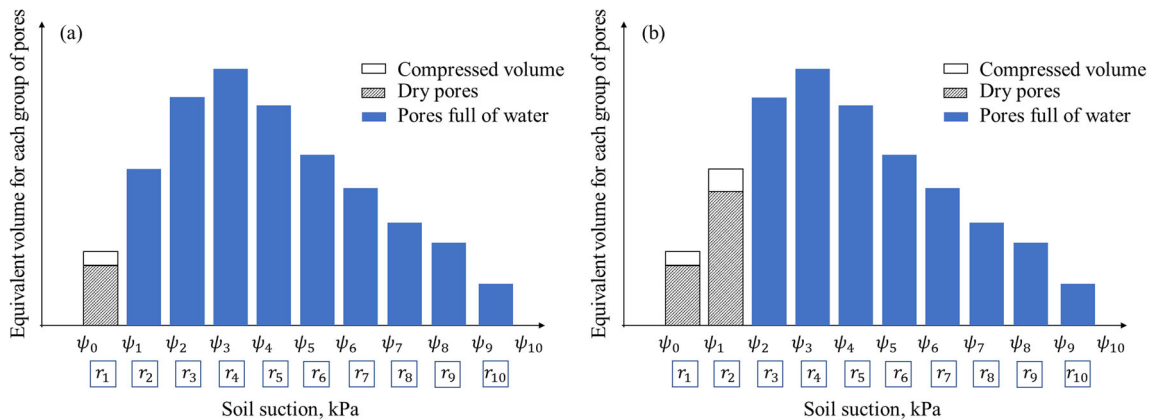


Fig. 3 Illustration of the drying process when the suction increases from ψ_0 to ψ_2 . **a** Step of soil suction increases from ψ_0 to ψ_1 , **b** step of soil suction increases from ψ_1 to ψ_2

3.2 Pore volume change in the drying process

Based on the definition of the gravimetric water content, in the representative elemental volume (REV) the water amount in the soil can be calculated from the mass of the soil particles. During the drying process, the mass of the soil particles in the REV is not changed and the decrease in the gravimetric water content represents two portions such as (i) the compression of pores and (ii) the desaturation of the pores in the REV. The degree of saturation (S) can be calculated from the gravimetric water content (w) and the void ratio (e) by using Eq. (4) as follows:

$$S = \frac{G_s w}{e} \tag{4}$$

where S is the degree of saturation, G_s is the specific gravity of the soil particle, w is the gravimetric water content and e is the void ratio.

The desaturation of the pores can be estimated from the VSC and the decrease in the gravimetric water content can be directly obtained from SWCC- w . If the degree of saturation remains constant with a change in the soil suction, then the decrease in gravimetric water content represents the amount of pore compression in the REV.

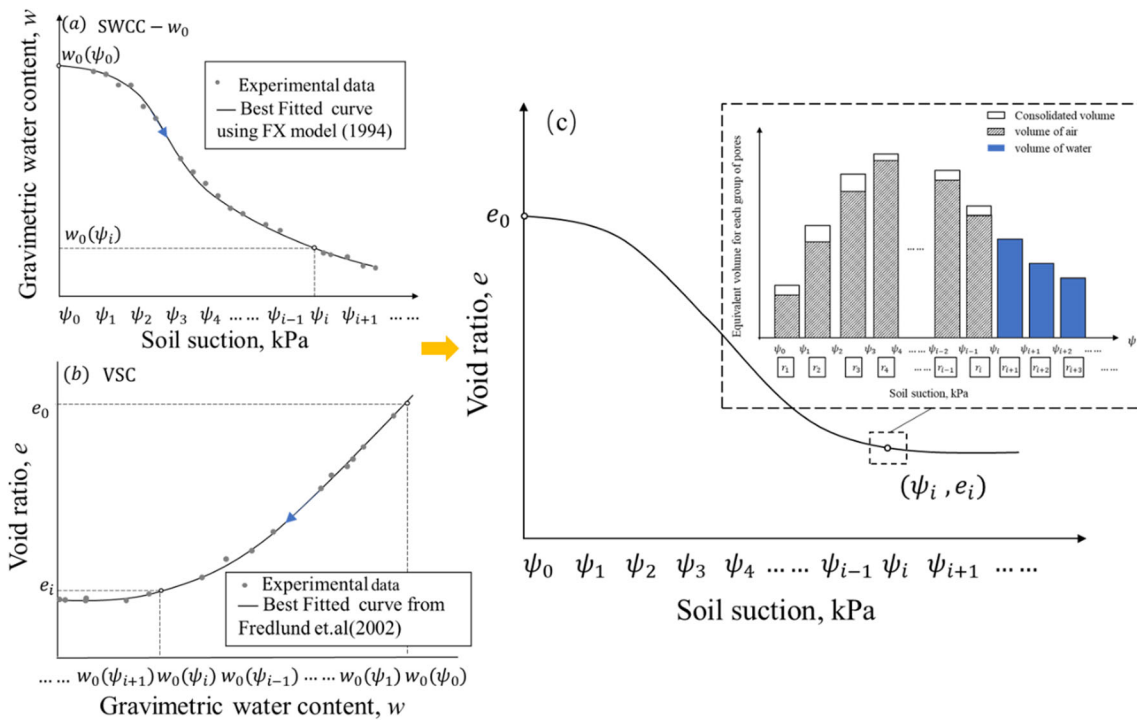


Fig. 4 Conversion of e -log (ψ) curve from SWCC- w_0 and VSC

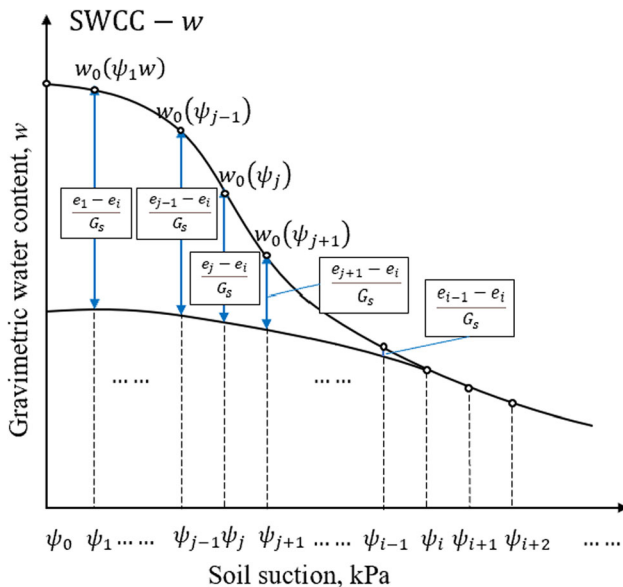


Fig. 5 Illustration of the calculation of SWCC- w_i for the suction less than ψ_i

Take the soil with void ratio of e_0 as the reference state, the PSDF of the soil corresponding to void ratio of e_0 is SWCC- S_0 . The pores in the REV can be divided into several fractions as shown in Fig. 2. Define the total volume of all the pores in the REV as 1, then the area of the columns in Fig. 2 represents the pore size density.

Table 1 Index properties of three types of soils selected in this paper

	Oil sands tailings	Regina clay	Maryland clay
Specific gravity, G_s	2.4	2.83	2.68
Liquid limit (LL), %	55	50	64
Plastic limit (PL), %	22	25	24

When the suction increases from ψ_{i-1} to ψ_i , the void ratio e_{i-1} will decrease to e_i , which can be calculated directly from the SWCC- w and VSC. The volume change of pores in the REV could be subsequently obtained from e_{i-1} and e_i , as illustrated in Eq. (5).

$$\Delta V_i = V_s(e_{i-1} - e_i) \tag{5}$$

where ΔV_i is the pore volume change in REV when the soil suction increases from ψ_{i-1} to ψ_i , e_{i-1} and e_i are the void ratios of soil corresponding to soil suction of ψ_{i-1} and ψ_i , respectively, V_s is volume of soil solids in the REV.

Figure 3 illustrates an example of drying process when the soil suction increases from ψ_0 to ψ_2 , which can be represented by two steps such as ψ_0 to ψ_1 and ψ_1 to ψ_2 . In each step, the decrease in gravimetric water content (which can be easily obtained from SWCC- w) can be divided into

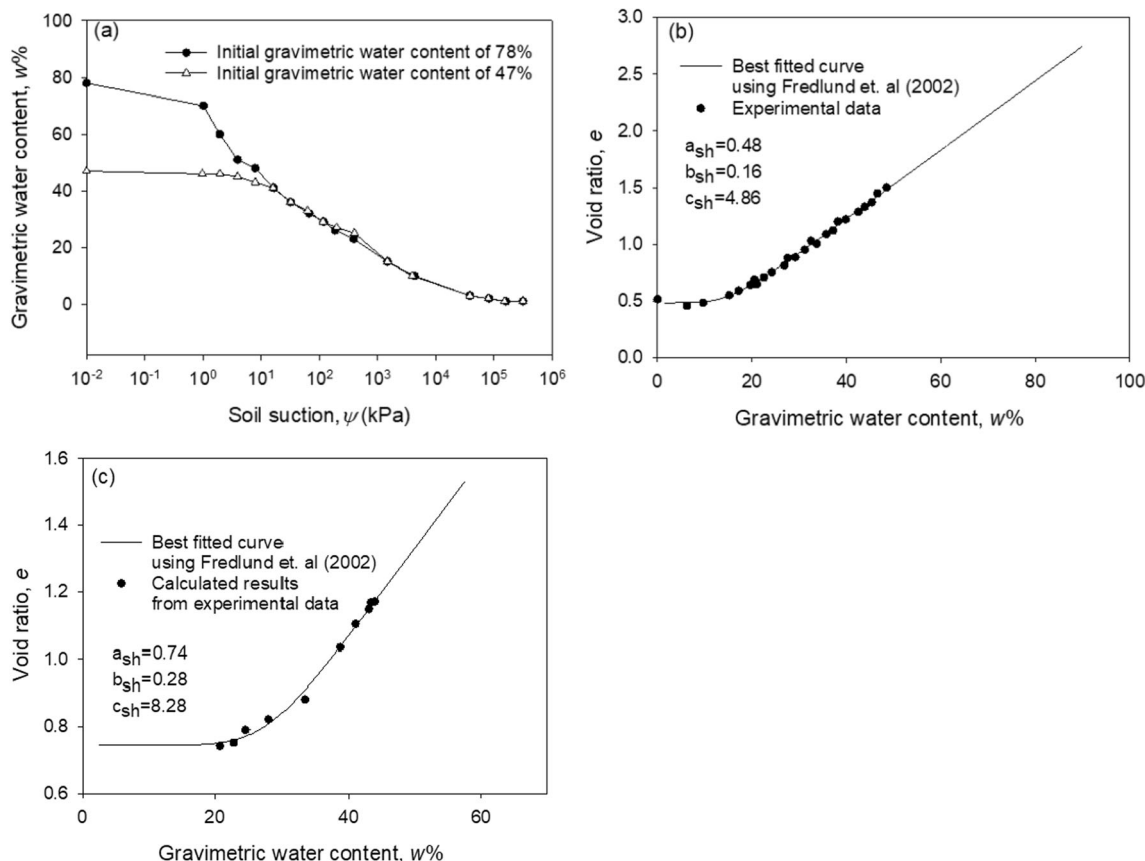


Fig. 6 Experimental data and best-fitted VSCs for three types of soils **a** Oil Sands tailings, **b** Regina clay and **c** Maryland clay

two portions including (i) compression of pores and (ii) the desaturation of the pores (or air volume in REV).

As illustrated in Fig. 3b, the compressed pore volume for each fraction can be estimated when the variation of void ratio is known. As a result, an updated PSDF at the instant of ψ_2 (with void ratio of e_2) can be calculated by recalculation of the pore size density for each fraction.

3.3 Procedures for calculating SWCC with initial void ratio of e_i

The SWCCs in the form of gravimetric water content for the specimens with initial void ratio of e_i and e_0 are defined as SWCC- w_i and SWCC- w_0 , respectively, while the volumetric shrinkage curve for the specimen with the initial void ratio of e_0 is defined as VSC. As a result, the e -log (ψ) curve can be obtained, as shown in Fig. 4, from SWCC- w_0 and VSC. By conducting the consolidation tests using both suction loading and the mechanical loading, Fredlund [3] observed that the soil deformation curve from the suction loading is similar to that from the mechanical loading. As a result, if the soil specimen remains under fully saturated condition, the pore size distribution for the specimen which is compressed by the suction loading would be same as that

of the specimen which is compressed to the same void ratio by the mechanical loading. In other words, when the soil suction increases beyond ψ_i , which is corresponding to e_i in e -log (ψ) curve in Fig. 4c, the SWCC- w for the specimen with the initial void ratio of e_i is same as that for the specimen with the initial void ratio of e_0 . As a result, it is crucial to estimate SWCC- w_i from both SWCC- w_0 and VSC for the suction range less than ψ_i .

The gravimetric water contents for the specimens with the initial void ratio of e_i and e_0 at the suction level of ψ_j are defined as $w_i(\psi_j)$ and $w_0(\psi_j)$, respectively. In the drying process, the soil is compressed (or e decreases) with the increase in soil suction. However, in the REV, both the volume (V_s) and the mass (M_s) of the soil particles are considered as incompressible. Then the water volume (ΔV_{water}) that drains out from the REV represents the compressed pore volume (ΔV_{pore}) and can be obtained from Eq. (6). Consequently, the variation in the gravimetric water content (Δw) can be obtained from Eq. (7).

$$\Delta V_w = \Delta V_{pore} = V_s \Delta e \tag{6}$$

$$\Delta w = \frac{\rho_w \Delta V_w}{M_s} = \frac{\rho_w V_s \Delta e}{\rho_s V_s} = \frac{\Delta e}{G_s} \tag{7}$$

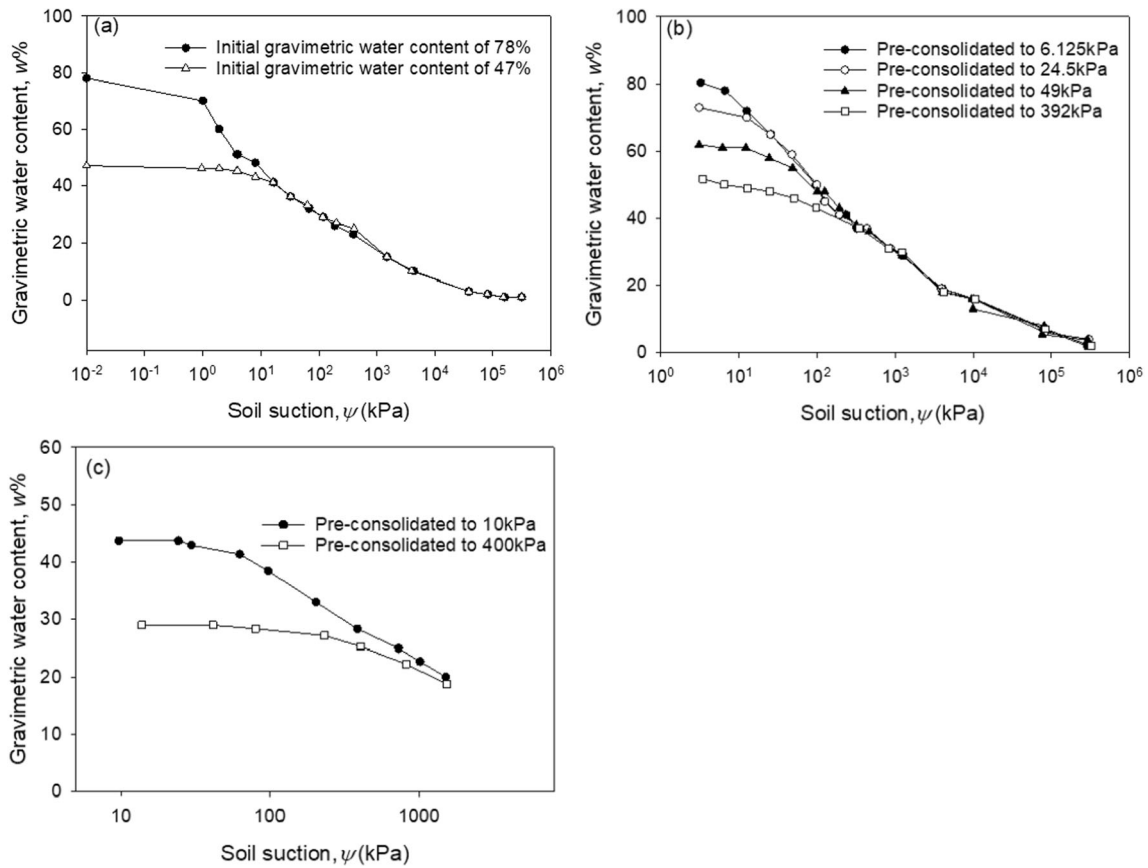


Fig. 7 Measured SWCCs-*w* for the soils with different initial void ratios. **a** Oil Sands tailings, **b** Regina clay and **c** Maryland clay

Table 2 Calculated $w_0(\psi)$ and e at different points for three types of soils

S	Matric suction, kPa	Oil sands tailings		Regina clay		Maryland clay	
		e	w (%)	e	w (%)	e	w (%)
Point 1	2.51	1.43	58.51	2.42	79.25	1.18	44.08
Point 2	6.31	1.24	50.58	2.35	77.02	1.174	44.01
Point 3	15.85	1.04	42.31	2.18	71.30	1.167	43.73
Point 4	39.815	0.85	34.73	1.86	60.86	1.14	42.50
Point 5	100.00	0.70	28.36	1.50	48.95	1.03	38.43
Point 6	251.19	0.58	23.21	1.20	39.35	0.87	31.38
Point 7	630.96	0.48	18.97	0.99	32.23	0.78	25.09
Point 8	1584.89	0.41	15.29	0.82	26.46	0.751	20.37
Point 9	3981.07	0.37	12.00	0.68	21.33	0.746	16.44
Point 10	10000.00	0.34	9.09	0.57	16.67	0.745	12.93
Point 11	25118.86	0.34	6.60	0.51	12.49	0.745	9.77
Point 12	63095.73	0.33	4.51	0.49	8.79	0.745	6.95
Point 13	158489.32	0.33	2.75	0.48	5.53	0.745	4.41
Point 14	398107.17	0.33	1.26	0.48	2.62	0.745	2.11
Point 15	1000000.00	0.33	0	0.48	0	0.745	0

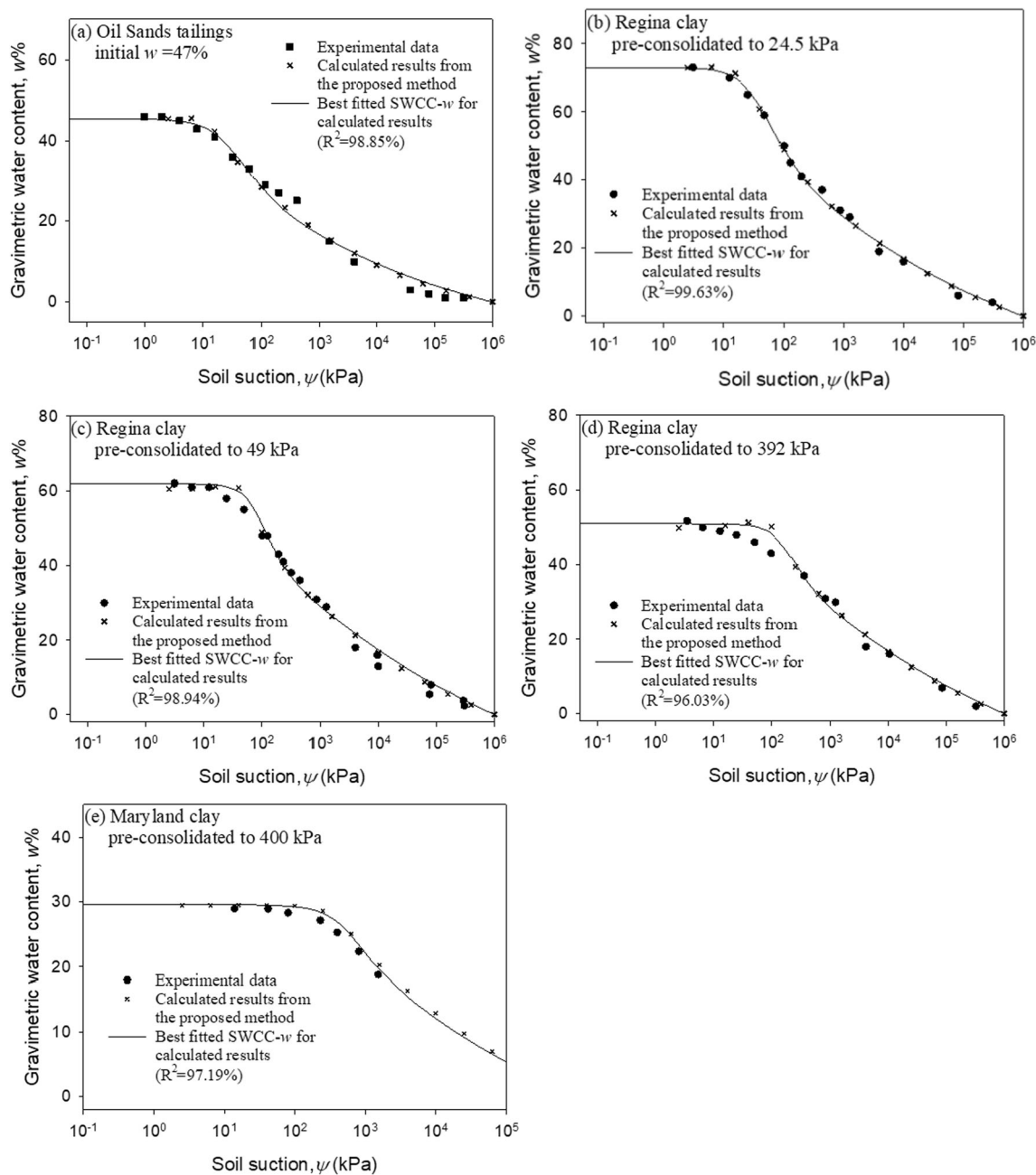


Fig. 8 Comparisons between the estimated SWCCs- w for the soils with different initial void ratios. **a** for Oil Sands tailings with initial water content of 47%; **b** for Regina clay which is pre-consolidated to 24.5 kPa; **c** for Regina clay which is pre-consolidated to 49 kPa; **d** for Regina clay which is pre-consolidated to 392 kPa; **e** for Maryland clay which is pre-consolidated to 400 kPa

where ρ_w is the density of water, ρ_s is the density of soil solid and G_s is the specific gravity of soil.

Consequently, the $w_i(\psi_j)$ can be obtained from Eq. (8) as shown in Fig. 5.

$$w_i(\psi_j) = w_0(\psi_j) - \frac{(e_j - e_i)}{G_s} \tag{8}$$

where e_i and e_j are the void ratios corresponding to soil suction ψ_i and ψ_j as shown in Fig. 4c.

4 Verification using published experimental data

To verify the proposed method in this paper, the experimental data including both SWCC- w_0 and VSC are selected from the published literature. The Oil Sands tailings and Regina clay from Fredlund and Houston [9], and Maryland clay from Li et al. [14] were selected in this

Table 3 Fitting parameters of estimated SWCCs- w and R^2 for the soils

Soils	a_f (kPa)	n_f	m_f	C_r (kPa)	R^2 (%)
Oil Sands tailings (47%)	22.26	0.56	1.43	1500	98.62
Regina clay (24.5 kPa)	32.99	0.47	1.78	1500	99.63
Regina clay (49 kPa)	65.91	0.47	2.89	1500	98.94
Regina clay (392 kPa)	83.94	0.56	0.81	1500	96.03
Maryland clay (400 kPa)	445.02	0.26	2.34	1500	97.19

paper. The index properties of these three types of soil are illustrated in Table 1.

Fredlund et al.'s equation [7] was adopted to best fit the the experimental data of VSCs for Oil Sands tailings, Regina clay and Maryland clay. The fitting parameters (a_{sh} , b_{sh} and c_{sh}) in Fredlund et al.'s equation [7] and the best-fitted curves are illustrated in Fig. 6. The experimental data of SWCC- w for these soils with different initial void ratios are shown in Fig. 7.

The SWCCs for the soil with the initial gravimetric water content of 78% for Oil Sands tailing, Regina clay pre-consolidated at 6.125 kPa and Maryland clay pre-consolidated at 10 kPa were selected as the SWCC- w_0 . Fifteen points at different suction levels were selected following the procedures as illustrated in Fig. 5. Both the w_0 (ψ) and e at different suction levels for those three types of soils are calculated and illustrated in Table 2. Subsequently, the values of w_0 (ψ) and e are used to calculate w_i (ψ), for the specimen with the initial void ratio of e_i . The comparison between the estimated results and the experimental data for those soils with different void ratios are illustrated in Fig. 8.

The Fredlund and Xing (1994)'s equation is used to best fit the calculated results, and the best-fitted SWCCs- w for those soils is obtained. The values of the fitting parameters and the coefficient of determination R^2 are illustrated in Table 3.

Table 3 and Fig. 8 indicate that the estimated SWCCs- w for those soils with different initial void ratios agree well with the experimental data. The values of determinations (R^2) for the estimated results from the proposed method in this paper are all larger than 96%, which indicate good performances in the prediction. Figure 8d shows that the estimated results are slightly higher than the measured results. This discrepancy may be resulted from the deformation of the soil particles, and in this paper, the soil particles are considered as incompressible.

5 Conclusion

In this paper, a new method is proposed for the prediction of the SWCCs- w for the fine-grained soil with different initial void ratios from a given SWCC- w_0 and VSC. In the proposed method, the measured data of drying SWCC- w_0 at the loose condition VSC in the drying process are used as the input in the proposed model. In the proposed model, the soil particles are considered to be incompressible during the shrinkage of soil sample. The predicted results from the proposed methods agree well with the experimental data for three types of soil from published literatures. The proposed method in this paper is proven to be a reliable method for the prediction of SWCCs- w of the fine-grained soil with different initial void ratios. The proposed method is straightforward and provides a convenient solution for obtaining SWCC for practical engineering purposes. The effect of the volumetric deformation of the clay particles on the variation of SWCC is not considered in this study. Further study is recommended on the volumetric deformation of the clay particles.

Acknowledgement The authors would like to acknowledge the financial supports he received from the National Natural Science Foundation of China (No. 52078128, 52178317), China Huaneng Group Co. Ltd. (No. HNKJ19-H17)

References

- Brooks RH, Corey AT (1964) Hydraulic properties of porous media. Hydrol paper no. 3. Colorado State University, Fort Collins, Colo
- Bate B, Nie S, Chen Z et al (2021) Construction of soil–water characteristic curve of granular materials with toroidal model and artificially generated packings. *Acta Geotech* 16:1949–1960
- Fredlund, D.G. (1964) Comparison of soil suction and one-dimensional consolidation characteristics of a highly plastic clay. National Research Council of Canada, Division of Building Research, Technical Report No. 245, Ottawa, Ontario, Canada
- Fredlund DG, Morgenstern NR, Widger A (1978) Shear strength of unsaturated soils. *Can Geotech J* 15:313–321
- Fredlund DG, Xing A (1994) Equations for the soil–water characteristic curve. *Can Geotech J* 31(3):521–532
- Fredlund DG, Xing A, Huang S (1994) Predicting the permeability function for unsaturated soils using the soil–water characteristic curve. *Can Geotech J* 31:533–546
- Fredlund MD, Wilson GW, Fredlund DG (2002) Representation and estimation of the shrinkage curve. In: Proceedings of 3rd international conference on unsaturated soils. UNSAT 2002, Recife, pp 145–149
- Fredlund MD (2010) User's manual for SVFlux, saturated-unsaturated numerical modeling. Soil Vision Systems, Saskatoon
- Fredlund DG, Houston SL (2013) "Interpretation of soil-water characteristic curves when volume change occurs as soil suction is changed" advances in unsaturated soils—proceedings of the 1st pan-American conference on unsaturated soils, PanAmUNSAT 2013. pp 15–31

10. Gallipoli D (2012) A hysteretic soil-water retention model accounting for cyclic variations of suction and void ratio. *Géotechnique* 62(7):605–616
11. Garakani AA, Haeri SM, Khosravi A, Habibagahi G (2015) Hydro-mechanical behavior of undisturbed collapsible loessial soils under different stress state conditions. *Eng Geol* 195:28–41
12. Habasimbi P, Nishimura T (2019) Soil water characteristic curve of an unsaturated soil under low matric suction ranges and different stress conditions. *Int J Geosci* 10(01):39–56
13. Lee IM, Sung SG, Cho GC (2005) Effect of stress state on the unsaturated shear strength of a weathered granite. *Can Geotech J* 42(2):624–631
14. Li J, Sun D, Sheng D, Sloan S, Fredlund DG (2007) Preliminary study on soil water characteristics of Maryland clay. In: 3rd Asian conference on unsaturated soils. Science Press, Beijing, pp 569–574
15. Millington RJ, Quirk JP (1961) Permeability of porous media. *Nature* 183(4658):387–388
16. Mualem Y (1976) A new model for predicting the hydraulic conductivity of unsaturated porous media. *Water Resour Res* 12(3):513–522
17. Millard A, Bond A, Nakama S, Zhang C, Barnichon JD, Garitte B (2013) Accounting for anisotropic effects in the prediction of the hydro-mechanical response of a ventilated tunnel in an argillaceous rock. *J Rock Mech Geotech Eng* 5(2):97–109
18. Nowamooz H, Masroufi F (2010) Suction variations and soil fabric of swelling compacted soils. *J Rock Mech Geotech Eng* 2(2):129–134. <https://doi.org/10.3724/sp.j.1235.2010.00129>
19. Ng CWW, Pang YW (2000) Influence of stress state on soil-water characteristics and slope stability. *J Geotech Geoenviron Eng* 126(2):157–166
20. Pasha A, Khoshghalb A, Khalili N (2020) Evolution of isochoric water retention curve with void ratio. *Comput Geotech* 122:103536. <https://doi.org/10.1016/j.compgeo.2020.103536>
21. Romero E, Della Vecchia G, Jommi C (2011) An insight into the water retention properties of compacted clayey soils. *Géotechnique* 61(4):313–328
22. Rostami A, Habibagahi G, Ajdari M, Nikooee E (2015) Pore network investigation on hysteresis phenomena and influence of stress state on the SWRC. *Int J Geomech* 15(5):04014072. [https://doi.org/10.1061/\(ASCE\)GM.1943-5622.0000315](https://doi.org/10.1061/(ASCE)GM.1943-5622.0000315)
23. Sun WJ, Cui YJ (2018) Investigating the microstructure changes for silty soil during drying. *Géotechnique* 68(4):370–373
24. Tarantino A (2009) A water retention model for deformable soils. *Géotechnique* 59(9):751–762
25. Tang CS, Shi B, Liu C, Suo WB, Gao L (2011) Experimental characterization of shrinkage and desiccation cracking in thin clay layer. *Appl Clay Sci* 52(1):69–77
26. Tavakoli Dastjerdi MH, Habibagahi G, Nikooee E (2014) Effect of confining stress on soil water retention curve and its impact on the shear strength of unsaturated soils. *Vadose Zone J* 13(5):1–11
27. van Genuchten MT (1980) A closed-form equation for predicting the hydraulic conductivity of unsaturated soils. *Soil Sci Soc Am J* 44:892–898
28. Vanapalli SK, Fredlund DG, Pufahl DE (1999) The influence of soil structure and stress history on the soil–water characteristics of a compacted till. *Géotechnique* 49(2):143–159. <https://doi.org/10.1680/geot.1999.49.2.143>
29. Yan W, Birle E, Cudmani R (2021) A new framework to determine general multimodal soil water characteristic curves. *Acta Geotech* 16:3187–3208
30. Zhang L, Chen Q (2005) Predicting bimodal soil–water characteristic curves. *ASCE J Geotech Geoenviron Eng* 131(5):666–670
31. Zhai Q, Rahardjo H (2015) Estimation of permeability function from soil water characteristic curve. *Eng Geol* 199:148–156
32. Zhai Q, Rahardjo H, Satyanaga A (2017) Effect of bimodal soil-water characteristic curve on the estimation of permeability function. *Eng Geol* 230:142–151
33. Zhai Q, Rahardjo H, Satyanaga A, Dai GL (2019) Estimation of unsaturated shear strength from soil-water characteristic curve. *Acta Geotech* 14(6):1977–1990
34. Zhai Q, Rahardjo H, Satyanaga A, Dai GL (2019) Role of pore-size distribution function on the water follow in soil. *J Zhejiang Univ Sci A* 20(1):10–20
35. Zhai Q, Rahardjo H, Satyanaga A, Dai GL, Zhuang Y (2020) Framework to estimate the soil-water characteristic curve for the soil with different void ratios. *Bull Eng Geol Env* 79:4399–4409

Publisher's Note Springer Nature remains neutral with regard to jurisdictional claims in published maps and institutional affiliations.

Springer Nature or its licensor (e.g. a society or other partner) holds exclusive rights to this article under a publishing agreement with the author(s) or other rightsholder(s); author self-archiving of the accepted manuscript version of this article is solely governed by the terms of such publishing agreement and applicable law.